Chapter 8
Earth System Dynamics Beyond the Second Law: Maximum Power Limits, Dissipative Structures, and Planetary Interactions

Axel Kleidon, Erwin Zehe, Uwe Ehret and Ulrike Scherer

Abstract Planet Earth is a thermodynamic system far from equilibrium and its functioning—obviously—obeys the second law of thermodynamics, at the detailed level of processes, but also at the planetary scale of the whole system. Here, we describe the dynamics of the Earth system as the consequence of sequences of energy conversions that are constrained by thermodynamics. We first describe the well-established Carnot limit and show how it results in a maximum power limit when interactions with the boundary conditions are being allowed for. To understand how the dynamics within a system can achieve this limit, we then explore with a simple model how different configurations of flow structures are associated with different intensities of dissipation. When the generation of power and these different configuration of flow structures are combined, one can associate the dynamics towards the maximum power limit with a fast, positive and a slow, negative feedback that compensate each other at the maximum power state. We close with a discussion of the importance of a planetary, thermodynamic view of the whole Earth system, in which thermodynamics limits the intensity of the dynamics, interactions strongly shape these limits, and the spatial organization of flow represents the means to reach these limits.

A. Kleidon (✉)
Max-Planck-Institute for Biogeochemistry, Hans-Knöll-Strasse 10, 07745 Jena, Germany
e-mail: akleidon@bgc-jena.mpg.de

E. Zehe · U. Ehret · U. Scherer
Institute of Water Resources and River Basin Management Karlsruhe Institute of Technology KIT, Kaiserstrasse 12, 76129 Karlsruhe, Germany
e-mail: erwin.zehe@kit.edu

U. Ehret
e-mail: uwe.ehret@kit.edu

U. Scherer
e-mail: ulrike.scherer@kit.edu

R. C. Dewar et al. (eds.), *Beyond the Second Law*,
Understanding Complex Systems, DOI: 10.1007/978-3-642-40154-1_8,

8.1 Introduction

Heat flows from warm to cold, water flows from the mountain top to the valley floor and wood burns into ashes. The reverse direction for these processes does not quite make sense. Heat does not spontaneously flow from cold to warm, water does not flow uphill, and wood does not emerge from the ashes. These directions reflect the fundamental direction imposed by the second law of thermodynamics. Yet, at the same time, this implication is almost trivial, in the sense that nobody would seriously question these directions as this is what we observe in nature over and over again. In this respect, the second law does not seem to contain much value to learn more about these processes because this knowledge is already established in the many mathematical descriptions we use to describe Earth system processes. So the basic question is whether there is more to learn from the second law of thermodynamics beyond these general trivialities?

The proposed principle of Maximum Entropy Production (MaxEP) seems to suggest that there is more to learn. The MaxEP principle states that processes do not merely follow the second law, but proceed at a maximum rate at which the rate of entropy production is maximized. This would essentially mean that the dynamics of isolated systems do not merely evolve towards a state of thermodynamic equilibrium, but that they would do so at the fastest possible rate. At the core of the thermodynamic interpretation of MaxEP is a trade-off, by which a greater flux is associated with a more depleted gradient. Since entropy production is expressed by the product of flux and gradient, the trade-off between flux and gradient results in a state of maximum entropy production at intermediate values for the flux and gradient. Over the last 15 years, renewed attention has been given to this principle, in terms of its theoretical basis [1–5] as well as its application to Earth and environmental processes [6–8]. While there are some indications for support, e.g. regarding heat transport by planetary atmospheres in simple climate models [9, 10] as well as general circulation models [11, 12], there are also quite a number of issues that still need to be resolved [13–15]. For instance, why should environmental systems "care" about entropy production, rather than more traditional quantities such as mechanical forces or mass fluxes? How would systems know that they "need" to maximize entropy production? With the breadth of competing processes shaping the Earth system, how do we know which entropy production should be maximized? And what new insights can be provided by MaxEP or similar maximization principles that we cannot get without these principles?

In this chapter we provide a brief overview of how these shortcomings of the proposed MaxEP principle can be overcome by shifting the focus onto the maximization of power, i.e. work through time, within an Earth system context. This maximization of power yields states that are nearly indistinguishable from equivalent MaxEP states, but it provides a clearer basis to understand which aspect is maximized within a system and to understand how this maximization is achieved. To do so, we first derive the Carnot limit from the laws of thermodynamics and then relate it to the maximum power limit in the next section. Then we

illustrate how maximization can be achieved by the organization of flow and how it relates to basic feedbacks that shape the evolutionary dynamics. This is then applied to the Earth system at large to explain how the dynamics and couplings of the planet essentially reflect the acceleration of the second law at the planetary scale. We close with a brief summary and conclusions.

8.2 Maximum Power Limits

Thermodynamics informs us about the limits of how much work can be derived from a heating gradient. The best known limit is the Carnot limit, which represents the best case for extracting work from a heating gradient that satisfies the first and second law of thermodynamics. For its derivation, we consider a system shown in Fig. 8.1a as a dashed box labeled "heat engine" that is situated between a hot reservoir with temperature T_h and a cold reservoir with temperature T_c. Applied to this setting, the first law in a steady state in which the internal energy does not change in time is represented by the balance of the heating by the heat flux J_{in}, the cooling by J_{out}, and the mechanical work done through time (or power), P_{ex}:

$$0 = J_{in} - J_{out} - P_{ex} \tag{8.1}$$

To identify the constraints imposed by the second law, we need to consider the entropy balance of the system . When we consider this balance in a steady state in which the entropy of the system does not change in time, this balance is represented by the entropy production due to irreversible processes within the system, σ, the entropy import by heating, J_{in}/T_h, and the entropy export by cooling, J_{out}/T_c:

$$0 = \sigma + \frac{J_{in}}{T_h} - \frac{J_{out}}{T_c} \tag{8.2}$$

The second law requires that $\sigma \geq 0$. With this requirement, we can combine Eqs. (8.1) and (8.2) and solve for P_{ex}:

$$P_{ex} \leq J_{in} \frac{T_h - T_c}{T_h} \tag{8.3}$$

The best case is given when the power equals the right hand side of this equation and this is known as the Carnot limit. It expresses the maximum rate by which heat can be converted into mechanical work that is permitted by the first and second law. Greater values of $P_{ex} = J_{in} - J_{out}$ would require $\sigma < 0$ in Eq. (8.2), which would violate the second law. Such conditions are shown in the upper right in Fig. 8.1a by the shaded area.

In this derivation of P_{ex}, it is assumed that no entropy is associated with P_{ex}, so that all of P_{ex} is associated with performing work. In the Earth system, such work is needed, for instance, to generate kinetic energy associated with motion, or to lift

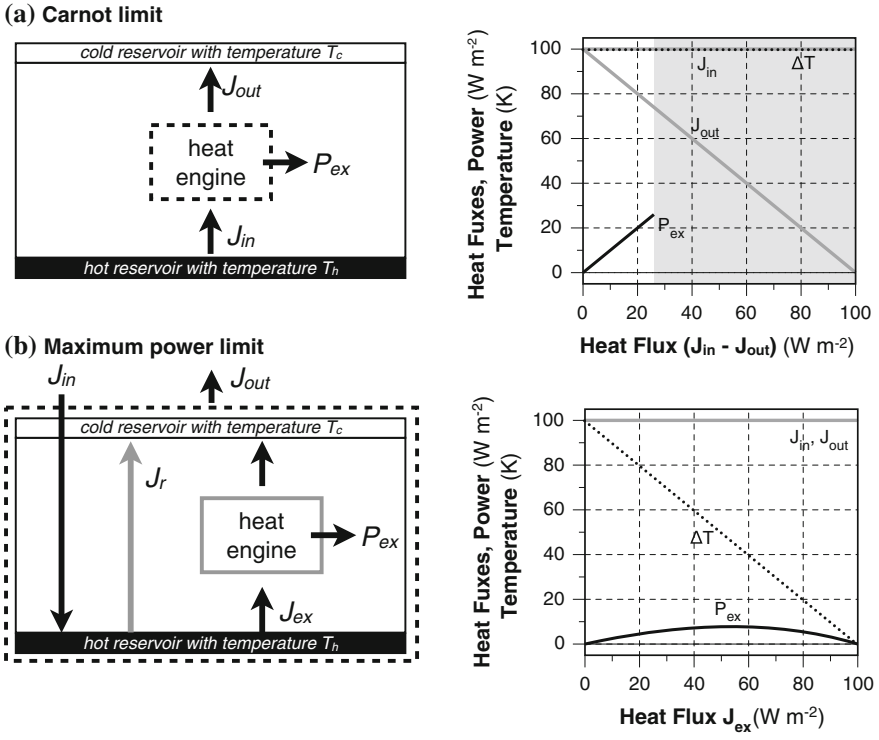

Fig. 8.1 Systems used in the text to describe **a** the Carnot limit and **b** the maximum power limit. The *dashed line* in the figures on the *left* show the delineation of the system boundary. The *right panels* show the sensitivity of the heat fluxes J_{in} and J_{out}, the temperature gradient $\Delta T = T_h - T_c$ and the extracted power P_{ex} to the heat flux utilized by the engine. The area *shaded grey* in the *upper right* plot shows conditions that is not permitted by the second law as it would require negative entropy production within the system, so that the Carnot limit of maximum power in the upper system is located at the edge of the *shaded* area. In the system shown in **b**, the maximum power limit results from the trade-off between a greater heat flux J_{ex} and the reduced temperature difference ΔT. After [17]

material against gravity and generate potential energy. We will refer to the generated form of energy as "free energy" here in a general sense because it is equivalent to the capacity of a system to perform work. The free energy is associated with a gradient of a different variable. For instance, when work is performed to generate motion, the form of free energy is kinetic energy, and the associated gradient is in the associated momentum. Hence, the Carnot limit can be seen as the maximum rate by which a heating gradient can be converted into a gradient of another variable.

The derivation of the Carnot limit makes two, important assumptions: (1) the two heat reservoirs that drive the heat engine remain at fixed temperatures and are not affected by the generation of work within the system; and (2) no irreversible

process takes place within the system. These assumptions cannot be made for many Earth system processes. Atmospheric convection, for instance, is driven by the heating associated with the absorption of solar radiation at the surface and the cooling aloft through the emission of terrestrial radiation. The convective motion transports about 99 W m^{-2} from the surface to the atmosphere in the global mean [16], which is more than half of the surface solar radiative heating of 160 W m^{-2}. Hence, the surface temperature is not a fixed boundary condition that drives the convective heat engine, but it is strongly affected by the intensity of convective cooling. In addition to this convective cooling, the surface is cooled by the net emission of terrestrial radiation of about 61 W m^{-2}, which is associated with irreversible radiative transfer that produces considerable entropy. Hence, the assumption that no entropy is produced is not fulfilled either. Similar arguments can be made for the large-scale poleward transport of heat by the climate system as well as for other processes, e.g. mantle convection in the Earth's interior. It would thus seem that the assumptions being made to derive the Carnot limit would not apply to quite a range of Earth system processes while the laws of thermodynamics naturally apply and limit the rate at which these processes can perform work.

We can nevertheless derive a maximum power limit for a slightly altered setup as shown in Fig. 8.1b that is more representative of Earth systems [17]. The two differences to the typical Carnot limit are that (1) the heat balances for T_h and T_c are part of the system and can therefore react to the rate at which work is performed within the system, and that (2) there is an additional process (radiative transfer, J_r, in Fig. 8.1b) that depletes the temperature gradient and produces entropy within the system. In this setup, we can use the steady-state surface energy balance (i.e. $dT_h/dt = 0$) as a constraint to express the temperature gradient $T_h - T_c$ as a function of the surface solar radiative heating, J_{in}, and the convective heat flux J_{ex} utilized by the convective heat engine:

$$0 = J_{in} - k_r(T_h - T_c) - J_{ex} \tag{8.4}$$

For simplicity, the net radiative exchange between the reservoirs is represented in a linearized way by $J_r = k_r(T_h - T_c)$, which is derived from the linearization of the Stefan-Boltzmann law.

To derive the maximum in power that can be derived from the heating difference $T_h - T_c$, we apply the Carnot limit to J_{ex}, use Eq. (8.4) to express $T_h - T_c$ in terms of J_{in} and J_{ex}, and get an expression of power P_{ex} that depends quadratically on J_{ex}:

$$P_{ex} = J_{ex}\frac{T_h - T_c}{T_h} = J_{ex}\frac{(J_{in} - J_{ex})}{k_r T_h} \tag{8.5}$$

When we neglect the dependence of T_h on J_{ex} in the denominator, this expression achieves a maximum value $P_{\max}$ for a convective heat flux $J_{ex} = J_{in}/2$ of

$$P_{\max} = \frac{J_{in}^2}{4k_r T_h} = \frac{1}{4} J_{in} \frac{T_{h,0} - T_{c,0}}{T_h} \tag{8.6}$$

where $T_{h,0}$ and $T_{c,0}$ are the temperatures for $J_{ex} = 0$.

The maximum power limit expressed in Eq. (8.6) looks like a Carnot limit [cf. Eq. (8.3), in particular when approximating $T_h \approx T_{h,0}$] with fixed, radiative equilibrium temperatures, except that it is reduced by a factor of 4. This reduction can directly be seen when comparing the maximum values of P_{ex} in Fig. 8.1a and b. The lower limit results from the reduction of the temperature gradient to half its maximum value and from the "competing" process of radiative transfer that consumes some of the heat flux J_{in}. This expression is essentially identical to the maximum power limit that is well known in electrical engineering and, when applied to typical atmospheric conditions, yields maximum estimates of power involved in atmospheric motion that are consistent with observations [17].

The maximum power limit is nearly identical to the Maximum Entropy Production (MaxEP) state reported earlier in atmospheric applications [9, 18]. This can be seen when considering the entropy budget of the system. In steady state, this budget is given by the import of entropy associated with the absorption of J_{in} at a temperature T_h, and the export of entropy associated with the emission of $J_{out} = J_{in}$ at a temperature T_c. The entropy production within the system due to radiative exchange, σ_r, and due to the convective heat flux, σ_{ex}, is balanced by the net entropy export by the system, so that

$$0 = \sigma_r + \sigma_{ex} + \frac{J_{in}}{T_h} - \frac{J_{in}}{T_c} \tag{8.7}$$

Noting that $J_{in} = J_r + J_{ex}$ and $\sigma_r = J_r(1/T_c - 1/T_h)$, we obtain

$$\sigma_{ex} = J_{ex}\left(\frac{1}{T_c} - \frac{1}{T_h}\right) = J_{ex}\frac{T_h - T_c}{T_h T_c} = \frac{P_{ex}}{T_c} \tag{8.8}$$

where we used the expression of P_{ex} from Eq. (8.5). In steady state, power equals dissipation, $P_{ex} = D$, in this closed system, so that the maximum power limit is equivalent to the maximization of σ_{ex} if all of the mechanical energy generated by P_{ex} is dissipated at the temperature T_c of the cold reservoir. This is typically not the case for the Earth's atmosphere. About half of the generated kinetic energy is either dissipated near the heated surface or is transferred into the ocean. Hence, the maximum power limit should be slightly below the MaxEP state. Nevertheless, the difference is hardly distinguishable using realistic numbers, so that the examples that provide support for the MaxEP principle concerning atmospheric heat transport [9–12], can equally be interpreted as an indication that the atmospheric circulation operates very close to the maximum power limit.

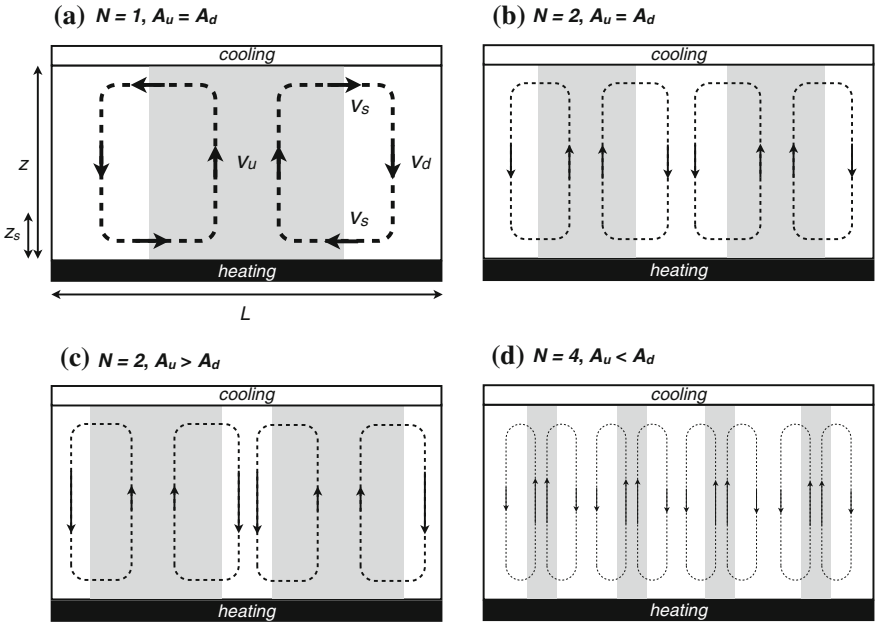

Fig. 8.2 Four examples of different flow structures that differ in the number of convection cells N and the areas of updraft A_u (*shaded grey*) in relation to the area of downdraft A_d of each cell. These different arrangements result in different intensities of frictional dissipation

8.3 Maximization Through Structure

The maximum power limit given by Eq. (8.6) establishes the upper limit to how much dynamics can be generated within a system, but it does not tell us how this maximization would be achieved, neither in terms of the evolutionary dynamics nor which aspect of motion would allow for the needed flexibility to achieve maximization. To explore the latter aspect (the former is dealt with in the next section), we need to look at how the flow is organized in space and time and how this organization affects the ability of the flow to generate and dissipate kinetic energy. This is done in the following using simple, conceptual considerations with some quantitative illustrations.

When motion is generated at a certain rate, the resulting flow can take various forms, as illustrated in Fig. 8.2. For instance, the flow can be accomplished by few, or many, convection cells N , and it can be associated with different areas over which updrafts take place. The physical balances that constrain these flow structures are the conservation of energy, mass and momentum, which apply to the local scale, but also at the global, system-level scale. At the local scale, momentum conservation leads to the well-known Navier–Stokes equation of fluid dynamics. What we aim for here is a system-level description of the dynamics that does not

require the information from the local scale, but only considers the balances at the global, aggregated level. The maximum power limit applied to the system level would then act as a constraint to the overall dynamics within the system. To understand how different flow configurations affect the system-level properties, particularly dissipation, we consider a simple, aggregated description of the system shown in Fig. 8.2 in the following.

The system depicted in Fig. 8.2 is a closed system that only exchanges heat with its environment. The dynamics of the total kinetic energy, A_{ke}, within the system then include only the generation and dissipation of kinetic energy, but does not include its exchange associated with mass exchange across the system boundary:

$$\frac{dA_{ke}}{dt} = P_{ex} - D \tag{8.9}$$

where P_{ex} is the generation rate of kinetic energy (being equivalent to the power of the heat engine from the previous section), and D is the rate of frictional dissipation. The main point about structure and maximization made here is that the many different ways in which the flow takes place (as, e.g., those shown in Fig. 8.2) are associated with different intensities of D, so that for the same P_{ex}, different values of A_{ke} can be achieved. Since a higher value of A_{ke} transports more heat, i.e. results in a greater value of J_{ex}, rearrangements in the flow can then form the basis for a positive feedback by which a higher value of A_{ke} results in a greater value of P_{ex} (which is explored further in the next section).

To demonstrate the different intensities of D associated with different flow patterns, we consider an area of size $A_{tot} = L^2$, where L is the horizontal dimension, a height of convection z and a boundary layer height of z_s. The updraft in each cell is assumed to take place with a uniform updraft velocity v_u through a horizontal, circular cross-sectional area of one updraft cell, $A_u = \pi r_u^2$, the downdraft takes place with a uniform downdraft velocity v_d and a cross-sectional area of $A_d = A_{tot}/N - A_u$, and a velocity v_s near the surface through a vertical, cylindrical cross-section at the bottom of the updraft cells of $A_s = 2\pi r_u z_s$.

Continuity requires that the mass fluxes J_m within a convection cell balance, i.e. that the mass lifted in the updraft is balanced by the mass transported by the downdraft and along the surface:

$$J_m = \rho A_u v_u = \rho A_d v_d = \rho A_s v_s \tag{8.10}$$

where we assume the same air density ρ for simplicity. This requirement yields the following expressions for the three velocities:

$$v_u = \frac{J_m}{\rho A_u} \qquad v_d = \frac{J_m}{\rho(A_{tot}/N - A_u)} \qquad v_s = \frac{J_m}{2\sqrt{\pi}\rho\sqrt{A_u} z_s} \tag{8.11}$$

noting that $r_u = \sqrt{A_u/\pi}$.

The total frictional dissipation D results from the friction within the fluid between the updrafts and downdrafts, D_a, from the contact with the surface, D_s,

and at the upper boundary at the top of the convection cell D_u, which we will assume to be equal to D_s for simplicity in the following (although friction at a solid surface may not be equal to internal friction within air):

$$D = D_a + 2D_s \tag{8.12}$$

Frictional dissipation within the fluid, D_a, is given by the viscosity of the fluid, μ, the velocity gradient between the cells, which is approximated by the difference in updraft- and downdraft velocities $(v_u - v_d)$ divided by the mean distance between the up- and downdraft within a cell, $L/2N$, through the vertical, cylindrical surface area of the updraft cell, $2\pi r_u(z - 2z_s)$:

$$\begin{aligned} D_a &= \mu\left(\frac{\partial v}{\partial x}\right)^2 A = \mu\left(\frac{v_u - v_d}{L/2N}\right)^2 (2\pi r_u)\,(z - 2z_s)N \\ &= \frac{\mu}{\rho^2}\gamma_a J_{m,tot}^2 \end{aligned} \tag{8.13}$$

where the geometric factor γ_a is given by

$$\gamma_a = 8\sqrt{\pi}\frac{A_{tot}}{A_u^{3/2}(A_{tot} - NA_u)^2}(z - 2z_s)N \tag{8.14}$$

In other words, the overall frictional dissipation within the fluid depends on material properties (viscosity μ and density ρ), the total mass flux $J_{m,tot} = NJ_m$ that is associated with the kinetic energy of convective motion, but also to some extent on a purely geometric factor, γ_a, that is associated with the organization of the mass flux in terms of the number of convection cells N as well as the cross section of the updraft A_u.

Frictional dissipation at the surface, D_s, is expressed similarly in terms of a velocity gradient, v_s/z_s, and the surface area, A_{tot}:

$$\begin{aligned} D_s &= \mu\left(\frac{v_s}{z_s}\right)^2 A_{tot} \\ &= \frac{\mu}{\rho^2}\gamma_s J_{m,tot}^2 \end{aligned} \tag{8.15}$$

where the geometric factor γ_s is given by

$$\gamma_s = \frac{1}{4\pi}\frac{A_{tot}}{A_u}\frac{1}{z_s^2}\frac{1}{N^2} \tag{8.16}$$

This expression is similar to Eq. (8.13) above in that it also depends on purely material properties, the total mass flux, as well as a geometric factor γ_s.

The total frictional dissipation D can then be expressed as:

$$D = \frac{\mu}{\rho^2}(\gamma_a + 2\gamma_s)J_{m,tot}^2 \propto \gamma A_{ke} \tag{8.17}$$

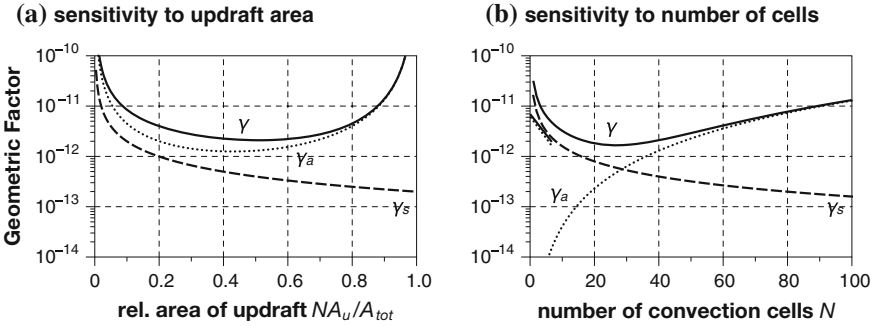

Fig. 8.3 Sensitivity of the geometric factors of flow organization related to interior friction within the fluid, γ_a, friction with the surface, γ_s, and total, $\gamma = \gamma_a + 2\gamma_s$, **a** to the total updraft area, NA_u/A_{tot} and **b** the number of convection cells, N. For both plots, the values $A_{tot} = 10^6$ m^2, $z = 1{,}000$ m, and $z_s = 100$ m are used. For the *left* plot a value of $N = 40$ was used, for the *right* plot a value of $NA_u/A_{tot} = 0.5$

which, by using the continuity requirement (Eq. 8.10), could be formulated in terms of the square of a velocity (e.g. v_u) to yield a typical parameterization for frictional dissipation, or in terms of the kinetic energy A_{ke} within the system.

Figure 8.3 shows the extent to which the total dissipation, D, depends on the flow configuration, as characterized by the geometric factors. As can be seen by the sensitivities, the geometric factors vary by an order of magnitude or more by the variation of A_u and N. Both sensitivities of the total geometric factor, $\gamma = \gamma_a + 2\gamma_s$, exhibit a characteristic minimum at which frictional dissipation is reduced merely by rearrangement of the flow.

As a consequence of this sensitivity of D to the arrangement of the flow, different values of the kinetic energy A_{ke} of the system can be achieved for the same generation rate P_{ex}. The critical link between this flexibility in A_{ke} and maximum power P_{ex} is that the amount of kinetic energy A_{ke} reflects the speed of motion within the convection cell, which in turn is related to the convective heat flux J_{ex} by

$$J_{ex} = c_p(T_h - T_c)J_{m,tot} \propto \Delta T\sqrt{A_{ke}} \tag{8.18}$$

In other words, a rearrangement in the flow can lower its frictional dissipation D (through the effect on γ in Eq. 8.17), enhance the flow velocity, transport more mass and heat (cf. Eq. 8.18), and thereby generate more power P_{ex} to drive the flow (cf. Eq. 8.5). This latter enhancement of P_{ex} through structured flow results from the concentration of the driving gradient at the boundary of the system (see also [19]). This effect can be seen by reformulating the expression of maximum power P_{ex} (Eq. 8.6) in terms of the temperature gradient by using the energy balance (Eq. 8.4):

$$P_{max} = \frac{k_r}{T_h}(T_h - T_c)^2 \tag{8.19}$$

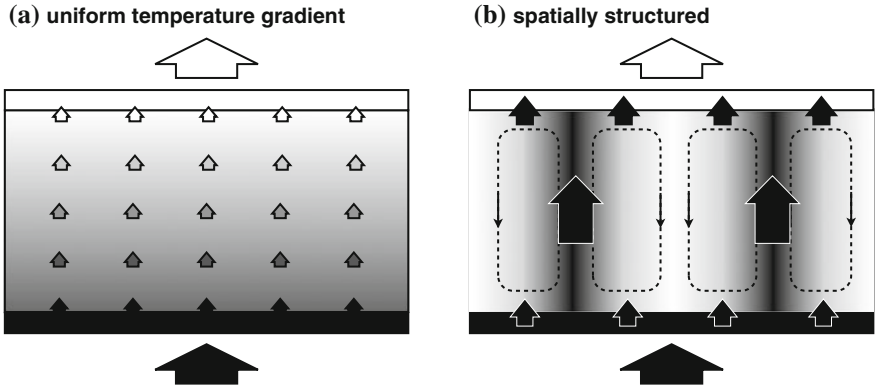

Fig. 8.4 Schematic illustration of the effect of structured flow on the distribution of temperature gradients. **a** In the absence of motion, the temperature gradient is uniformly distributed across the system between the heating source below, and the cooling source aloft. **b** When structured flow takes place, temperature gradients are confined to small regions at the interface to the heating and cooling source and are able to enhance the generation rate of motion

In other words, P_{max} depends quadratically on the temperature gradient. The implication of this is that for the same rate of heating, J_{in}, a uniform distribution of the temperature gradient yields less power than a non-uniform distribution of the gradient at the system boundary. This effect is qualitatively illustrated in Fig. 8.4. With stronger motion, more cooled air is advected by the convection cell to the heated surface, thereby concentrating the temperature gradient to the area near the surface. The key insight here is that a non-uniform distribution of the driving temperature gradient is intimately linked with the development of structured flow and that this affects the ability of the system to derive power from the temperature gradient.

Of course, this simple example makes several assumptions, such as constant density and a simple geometry, and treats convection in a highly simplistic way. It nevertheless substantiates the point that the formation of specific flow structures such as convection cells affect the *intensity* by which kinetic energy is dissipated and thereby constitute "degrees of freedom" that allow the fluid to adjust to a state of maximum power.

8.4 Dynamics and Feedbacks Associated with Maximization Through Structure

We now ask why the evolution and the dynamics of a system would inevitably evolve to a maximum power state. The following discussion on feedbacks show rather general mechanisms that, in principle, should be transferrable to very different structures as well (for instance water flow in river basin networks, [20]).

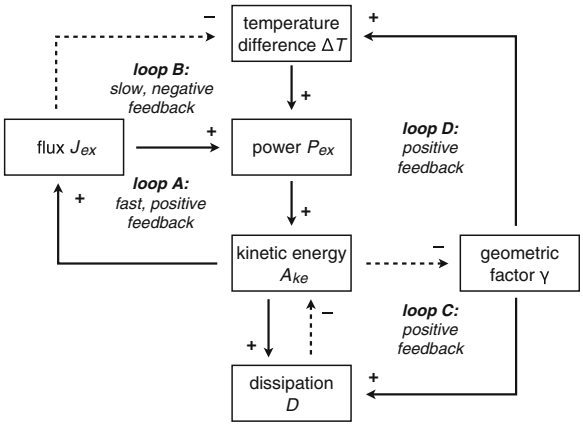

Fig. 8.5 A feedback diagram to illustrate how the dynamics of kinetic energy generation and dissipation relate to the maximization of power and structure formation. *Solid lines* with "+" indicate positive influences (e.g., a larger temperature difference results in a greater power, i.e. the derivative $\partial P_{ex}/\partial \Delta T > 0$). *Dashed lines* with "−" show negative influences (e.g., an enhanced heat flux reduces the driving gradient, i.e. $\partial \Delta T/\partial J_{ex} < 0$). Four feedback loops (A, B, C, D) are shown: Feedbacks A and B on the *left* relate to the maximum power limit, and the feedbacks C and D on the *right* relate to how structured flow can achieve this limit. After [20]

We illustrate these feedbacks in the following specifically with the example of convective motion given above, bringing together and summarizing the previous sections. We describe these feedbacks similar to the feedback analysis that is common in climatology [21].

Imagine if the system shown in Fig. 8.1b is initially at rest, i.e. in a state of no convective heat flux $(J_{ex} = 0)$ and no kinetic energy $(A_{ke} = 0)$. This state satisfies the energy-, mass-, and momentum balances of the system. We now need to understand why such a state, when perturbed, would evolve towards a dynamic state with $A_{ke} > 0$, and why this evolution would "stop" at a maximum power state. In the context of feedbacks, we need to identify a positive feedback that amplifies the growth of the initial perturbation, and a negative feedback that stops the growth at the maximum power state. Before we identify these feedbacks, let us first go through the relationships between the different variables of the system as shown in Fig. 8.5 and relate them to the above equations.

The source for the dynamics is the temperature difference $(\Delta T = T_h - T_c)$ in the system that develops due to the uneven heating and cooling of the system due to J_{in} and J_{out}. This gradient generates buoyancy and motion, and enters directly the expression for the generation rate of kinetic energy (P_{ex}, Eq. 8.5). This power (P_{ex}) generates kinetic energy (A_{ke}, Eq. 8.9), which is then subsequently dissipated (D). The rate of dissipation (D) depends on the kinetic energy (A_{ke}) as well as the spatial organization of the flow, characterized by the geometric factor γ (Eq. 8.17). Motion in the system results in the convective heat flux (J_{ex}), so that this heat flux depends on the kinetic energy A_{ke} and the temperature difference ΔT (Eq. 8.18).

The following feedbacks are established because the temperature difference (ΔT) as well as the power (P_{ex}) depend on the convective heat flux J_{ex} (Eqs. 8.4 and 8.5).

We now look at the consequences of a perturbation in the temperature difference ($d\Delta T$) on the generation of kinetic energy (dP_{ex}). The generation rate (P_{ex}) depends on the convective heat flux (J_{ex}) and on the temperature difference (ΔT), so that, effectively, $P_{ex} = P_{ex}(J_{ex}(A_{ke}(P_{ex}, D)), \Delta T_{ex})$. Hence, the overall change in dP_{ex} depends on the direct effect of ΔT on P_{ex} (i.e. $\partial P_{ex}/\partial \Delta T$), and indirect effects due to the various interdependencies, which are described by a product of partial derivatives

$$\frac{dP_{ex}}{d\Delta T} = \frac{\partial P_{ex}}{\partial J_{ex}} \frac{\partial J_{ex}}{\partial A_{ke}} \frac{\partial A_{ke}}{\partial P_{ex}} \frac{\partial P_{ex}}{\partial \Delta T} + \frac{\partial P_{ex}}{\partial \Delta T} \frac{\partial \Delta T}{\partial J_{ex}} \frac{\partial J_{ex}}{\partial A_{ke}} \frac{\partial A_{ke}}{\partial P_{ex}} \frac{\partial P_{ex}}{\partial \Delta T} \tag{8.20}$$

The first term on the right hand side represents a positive feedback (feedback A in Fig. 8.5). An increase in the generation rate results in an increase in kinetic energy ($\partial A_{ke}/\partial P_{ex} > 0$), which causes an increase in the heat flux ($\partial J_{ex}/\partial A_{ke} > 0$) which in turn results in greater power ($\partial P_{ex}/\partial J_{ex} > 0$). Since all derivatives are positive, the initial change is amplified and this constitutes a positive feedback. The second term on the right hand side represents a negative feedback (feedback B). The last three derivatives are the same as in the first term and describe the increase of the heat flux J_{ex} due to the initial change in ΔT. The greater heat flux also results in a decrease in the temperature difference ($\partial \Delta T/\partial J_{ex} < 0$), and a decrease in temperature difference decreases the power ($\partial P_{ex}/\partial \Delta T > 0$). Hence, the product of these derivatives is negative, so that these effects constitute a negative feedback. Since temperature changes involve changes in thermal inertia, this feedback is likely to act more slowly than feedback A.

With increasing values of kinetic energy (A_{ke}) in the system, the derivatives change their values, and so do the strengths of the two feedbacks. The deciding difference in these feedbacks relates to the terms $(\partial P_{ex}/\partial J_{ex})$ and $(\partial P_{ex}/\partial \Delta T)(\partial \Delta T/\partial J_{ex})$, while the other terms could be factored out in the above Eq. (8.20). Because $(\partial P_{ex}/\partial J_{ex}) = \Delta T/T_h$, $(\partial P_{ex}/\partial \Delta T) = J_{ex}/T_h$, and $(\partial \Delta T/\partial J_{ex}) = -1/k_r$, the sum of these terms $(\partial P_{ex}/\partial J_{ex}) + (\partial P_{ex}/\partial \Delta T)(\partial \Delta T/\partial J_{ex})$ decreases with an increasing values of J_{ex}, and cancel each other exactly at the maximum power state, when $\Delta T/T_h - J_{ex}/(k_r T_h) = 0$, or $J_{ex} = k_r \Delta T = J_{in}/2$. In other words, at the maximum power state, the feedbacks A and B operate with same strength, but with opposite signs, so that the maximum power state should be the state that is dynamically the most stable. Noting that power equals dissipation in steady state, this line of reasoning is consistent with the dynamic stability analysis of Malkus [22], with the derivation by Dewar and Maritan (Chap. 3), and with the reasoning behind the MaxEP state by Ozawa et al. [6].

The spatial organization of the flow affects the two feedbacks described above. In steady state, we have $P_{ex} = D \propto \gamma A_{ke}$, so that $A_{ke} \propto P_{ex}/\gamma$. Hence, the derivative $\partial A_{ke}/\partial P_{ex} \propto \gamma^{-1}$ depends on the spatial arrangement of the flow. To relate structure formation to the maximization of power, we note that changes in ΔT can also result from the internal dynamics and, specifically, the spatial organization as

shown in Fig. 8.4. The feedbacks that are related to structure formation are shown in Fig. 8.5 in terms of feedbacks C and D. Feedback C characterizes the reduction in frictional dissipation due to the development of structured flow that is captured by the geometric factor γ. In other words, when an increase in kinetic energy results in a change in spatial organization and a reduction in the geometric factor ($\partial\gamma/\partial A_{ke} < 0$), this would reduce dissipation ($\partial D/\partial\gamma > 0$), resulting in an increase in kinetic energy ($\partial A_{ke}/\partial D < 0$). Overall, this feedback constitutes a positive feedback related to the reduction of internal dissipation due to spatial reorganization of the flow. The implication of this feedback is that for a given generation rate P_{ex}, a reduction in γ would enhance A_{ke}, J_{ex}, and thus P_{ex}. Hence, those perturbations in the spatial organization of the flow that enhance power would continue to grow and play an important part of feedback A. The confinement of temperature gradients to the system boundary that was qualitatively discussed above constitutes a further feedback (feedback D, see also Schneider and Kay [19] for relevant discussion on temperature profiles in convective cells), in which a change in spatial organization would affect the temperature difference (ΔT), power (P_{ex}), kinetic energy (A_{ke}), which could then feed back to the value of the geometric factor. While we did not provide mathematical relationships to express this feedback in detail, these effects would be reflected in the partial derivatives of $\partial A_{ke}/\partial P_{ex}$ and $\partial\Delta T/\partial J_{ex}$, thereby affecting feedback B.

To sum up, this discussion on dynamics and feedbacks suggests that a state of maximum power would naturally emerge from the dynamics within a system. First, a fast, positive feedback enhances free energy generation within the system through the formation of structured flow. This positive feedback is eventually balanced by the development of a negative feedback associated with the depletion of the driving gradient through the enhanced heat transport, so that the dynamics should be maintained in a steady state near the maximum power limit.

8.5 Implications of Maximum Power for Planetary Interactions

When we apply maximum power limits to the Earth system, we need to recognize that essentially all forms of free energy originate directly or indirectly from the planetary drivers: solar radiation and the cooling of the Earth's interior. These maintain the ultimate driving gradients from which free energy is generated, which is then either dissipated directly, or converted into other forms of free energy and dissipated subsequently. For instance, heating gradients generated by differences in the absorption of solar radiation result in the generation of kinetic energy and associated momentum gradients. These gradients are either dissipated by friction, or used to dehumidify the atmosphere and lift water vapor to the height at which it condenses. Subsequently, surface evaporation dissipates the gradient in specific humidity and falling raindrops dissipate the potential energy. Hence, the dynamics

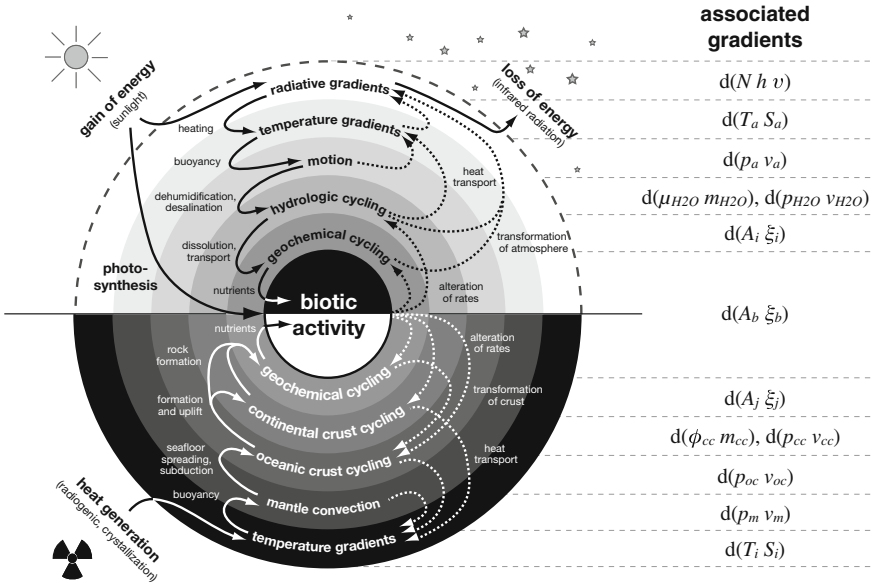

Fig. 8.6 Schematic diagram of the planetary hierarchy of free energy generation, transfer and dissipation to different forms (*solid lines*) and associated effects on the driving gradients (*dotted lines*). The different layers are associated with different forms of gradients, free energy and disequilibrium. The associated gradients that express these forms of free energy are shown on the right, with radiant energy expressed by the number of photons N, and the energy per photon hv with frequency v, thermal energy by temperature T and entropy S, kinetic energy by momentum p and velocity v, binding energy by chemical potential μ and mass m, potential energy by geopotential ϕ and mass m, and chemical energy by affinity A and extent of reaction ξ. After [37]

of the Earth system can be viewed as an interconnected cascade of energy conversions, as illustrated in Fig. 8.6.

The second law and the maximum power limit have five important, broader implications for the cascades of energy conversions within the Earth system:

Hierarchy of free energy generation and driving gradients. The generation of different forms of free energy within the Earth system do not take place independently, but the free energy and the associated gradients generated by one process typically form the driving gradient of another process. This connectedness of the free energy generation terms is shown by the solid lines in Fig. 8.6. For instance, the gradient $d(Nhv)$ in radiative exchange at the Earth-space boundary causes gradients in radiative heating, $d(TS)$, which is in part converted into the kinetic energy, $d(pv)$, associated with atmospheric motion and gradients in velocity v. Motion in turn is in part dissipated by friction, that is, kinetic energy $d(pv)$ is converted into heat $d(TS)$, but also performs other types of work, e.g. lifting dust and moisture or forming waves and currents in the ocean. These transfer processes generate potential energy, $d(\phi m)$, out of the kinetic energy of motion $d(pv)$. As a consequence, the dynamics of free energy are then not simply

formed by generation and dissipation terms, as it is often being done (e.g. in the form of the Lorenz energy cycle in atmospheric dynamics [23, 24], or as represented by the simple representation in Eq. 8.9 above), but include transfer terms to other forms of free energy. These transfer terms of energy play the critical role of the "glue" that connects processes and that in the end result in the highly complex and interacting Earth system. The formulation of these dynamics in terms of driving gradients and resulting forms of free energy provides a clear direction and causality despite the complexity that is involved.

Interactions and feedbacks to driving gradients at higher levels. When free energy is generated from a driving gradient, the driving gradient is inevitably depleted. In the simple example in Sect. 8.2, the generation of motion inevitably results in a convective heat flux that depletes the temperature gradient (as also shown in the feedbacks in Fig. 8.5). Consequently, each conversion along the solid lines shown in Fig. 8.6 is associated with inevitable effects on the driving gradients, as indicated by the dashed lines in Fig. 8.6, and therefore on the whole chain of conversions. For instance, when motion is generated by differential radiative heating, the resulting motion transports heat that accelerates the depletion of the differential radiative heating. When motion lifts vapor to greater heights and colder temperatures, it brings vapor to condensation. This dehumidification of the atmosphere by motion results in the transport of latent heat that reduces the heat available for driving the atmospheric heat engine [25–28]. Hence, each conversion along the solid lines in Fig. 8.6 results in inevitable interactions between processes that affect free energy generation by these processes and, ultimately, the exchange of radiation and entropy with space.

Maximum power limits. The conversions of gradients into different forms of free energy down the hierarchy shown by the solid lines in Fig. 8.6 is restricted by the rate by which the gradient is generated in the layer above. At best, all of the driving gradient can be converted into free energy. For most of the conversions, however, free energy can either be dissipated directly or converted into another form of free energy further down the layers and dissipated subsequently. These two "options" for the fate of the free energy imply maximum power limits akin to the one shown in Sect. 8.2 in which the direct dissipation is associated with radiative transfer (J_r), while the conversion to free energy and its subsequent dissipation is associated with P_{ex} and D, respectively. Consequently, each of the free energy conversions down from the planetary driver involves some direct dissipation, so that less free energy can be generated with each additional conversion.

What this then implies is that because of these limits, abiotic processes cannot generate substantial amounts of chemical free energy ($d(A_i\xi_i)$ and $d(A_j\xi_j)$ in Fig. 8.6) that could transform the chemical composition of the atmosphere. In contrast, photosynthetic life avoids these dissipative losses by generating chemical free energy ($d(A_b\xi_b)$ in Fig. 8.6) directly by exploiting $d(Nhv)$ by photochemistry. This insight is consistent with the common attribution of the chemical disequilibrium in the Earth's atmosphere to the presence of abundant life [29, 30]. By

formulating biotic activity in such thermodynamic terms, one may also explore maximum power limits in biochemical processes [31] and the biosphere [32, 33].

Maximization by dissipative structures. Maximization of the different rates of free energy conversions can take place by developing structures that are able to reduce the extent of internal friction and dissipation. While the maximum power limit is given by the constraints imposed by the driving gradient, this limit can only be achieved by adjustments of the dynamics associated with the generated form of free energy. This possibility of the flow to adjust its level of frictional dissipation was demonstrated in Sect. 8.3 for convective flow. The widespread presence of similar, reproducible structures, such as convection cells, waves or fractal networks in Earth system processes can be seen as the manifestation of maximization through structure at different spatial and temporal scales. This interpretation of dissipative structures as the means to achieve the maximum power limit provides a new and broader basis to link previous work along similar lines (e.g. Prigogine's "dissipative structures" [34], Bejan's "constructal law" [35] and the assumption of minimum energy dissipation in fractal networks by [36]) to the flexible boundary conditions and interactions within the planetary context.

The Second Law at the planetary scale. Each of the conversions of gradients among the different layers in Fig. 8.6 obey the second law, which is contained in the maximum power limit by the assumption that P_{ex} operates at the Carnot limit. In fact, the dynamics of free energy generation, transfer, and dissipation are such that they enhance gradient depletion and thereby accelerate processes in the direction of the second law when evaluated at the scale of the gradient that is at a higher layer within the hierarchy. In the simple example in Sect. 8.2 this acceleration is reflected in the depleted temperature gradient $T_h - T_c$, with a maximum possible reduction at the maximum power limit to $T_h - T_c = (T_{h,0} - T_{c,0})/2$. In the Earth's atmosphere, this depletion is reflected in the reduced gradient in the net radiative exchange at the top of the atmosphere as a result of large-scale atmospheric heat transport (which, in the context of the system described here, would correspond to spatial differences in $J_{in} - J_{out}$). When we generalize this effect and apply it to the planetary system, this would imply that the overall dynamics of free energy generation and transfer among the different layers in Fig. 8.6 are such that these deplete gradients faster, possibly as fast as possible (cf. "maximization by structure"), so that the whole system should deplete the driving, radiative gradients by as much as possible. This would then imply that the complex dynamics of the Earth system would result in the maximum rate of radiative entropy production to the extent that this is possible by the dynamics associated with free energy transformations. This latter restriction is important: The heat transport by convection, for instance, could not completely level out the temperature gradient (i.e. $T_h - T_c = 0$ cannot be achieved by the heat transported by motion in steady state) but is restricted to states below or at the maximum power limit in steady state (as discussed above in the context of feedbacks). This perspective of the hierarchy

shown in Fig. 8.6 as the implementation of a "planetary accelerator" of the second law provides a powerful general direction to the complex and seemingly arbitrary conversions and interactions within the Earth system.

8.6 Summary and Conclusions

In this chapter, we described how the second law of thermodynamics sets the direction and constraints for the dynamics of the whole Earth system, but also how the dynamics act to accelerate the second law towards a state of thermodynamic equilibrium. The sequence of generation, dissipation, and transfer of free energy to different forms acts to accelerate the progress into the direction imposed by the second law. At the same time, the second law imposes a fundamental constraint on the strength of this sequence by setting the maximum power limit. This limit can be achieved by the internal dynamics of the system through adjustments of the flow into structures, such as convection cells. The development of such "dissipative structures" reduces internal dissipation, so that for the same generation rate, more free energy can be maintained within the system. This results in a positive feedback that enhances free energy generation and structure formation up to the maximum power limit. At this limit, the negative feedback resulting from the accelerated depletion of the driving gradient compensates the positive feedback, resulting in dynamics that should be maintained near a steady state of maximum power.

When this perspective is applied to the dynamics of the Earth system as a whole, this results in a hierarchy of free energy generation and transfer, where one form of generated free energy constitutes the driving gradient for the generation of another form of free energy. Overall, such a planetary hierarchy of free energy conversions should represent a "planetary accelerator" towards a state of thermodynamic equilibrium and, when maintained at maximum power, reflect the means to deplete the planetary driving gradients as fast as possible. Since the Earth exchanges mostly radiation of different entropy with space, this would constitute the means to overall produce radiative entropy at the maximum possible rate by these dynamics that involve the conversions and dissipation of the various forms of free energy.

The thermodynamic limits in this chapter were formulated in terms of maximum power limits rather than in terms of the proposed principle of Maximum Entropy Production (MaxEP). The outcomes of both, maximum power or MaxEP, are essentially indistinguishable in terms of the associated temperature gradients and heat fluxes when applied to e.g. a convective system. The maximum power limit has the advantage that it specifically describes the driving gradient and the dynamical processes involved, which should facilitate the application of this limit to Earth system processes. In comparison, the use of MaxEP is often ambiguous because it is not clear which entropy production is to be maximized and why the dynamics would be such that they result in maximization of entropy production compared to other aspects that are more directly involved in the dynamics (such as

forces, energy or power). In this sense, the shift in focus to maximum power should not be seen as a contradiction to previous work on MaxEP, but rather as a continuation and sharpening of the application of thermodynamic limits to Earth system processes. It is quite likely that the maximization of power by systems can be derived as a form of entropy production maximization that is constrained by more than the energy- and mass balance, e.g. by the momentum balance [22] (Dewar and Maritan, Chap. 3). No matter whether power or entropy production is maximized, the key aspect in the maximization is that the boundary conditions are not fixed, but react to the dynamics within the system and accelerate the depletion of the driving gradient. Hence, the maximization reflects the central role of interactions between the system dynamics and the boundary conditions. The shift in emphasis from MaxEP to maximum power led to the insight that systems are able to adjust to maximum power states through the development of structured flow that reduces frictional dissipation within the system.

This perspective needs to be developed further in the future, as it allows us to become more specific regarding the conditions under which the maximum power state is achievable. For instance, the minimum dissipation solution in the example presented in Sect. 8.3 depends on the total size of the system (i.e. A_{tot}), while the value of N is constrained to integer values $N \geq 1$. Even in this simple example one can envision situations where the system is too small to be flexible enough to minimize internal dissipation and therefore being unable to evolve to the maximum power state. In such a case, the dynamics are too constrained, or, formulated differently, the degrees of freedom within the system are too low to achieve the maximum power state.

Overall, the progression presented here from a relatively simple MaxEP view of the dynamics of Earth system processes to "maximization of power through structure" within the context of the whole Earth system should provide a much more specific basis to demonstrate the relevance of thermodynamic limits to the structure and functioning of the planetary dynamics of the Earth system.

Acknowledgments This research contributes to the Helmholtz Alliance "Planetary Evolution and Life". The authors thank Roderick Dewar and two anonymous reviewers for their constructive comments.

References

1. Dewar, R.C.: Maximum Entropy Production and non-equilibrium statistical mechanics. In: Kleidon, A., Lorenz, R. D. (eds.) Non-Equilibrium Thermodynamics and the Production of Entropy: Life, Earth, and Beyond, pp. 41–56, Springer, Heidelberg (2005)
2. Dewar, R.C.: J. Phys. A **38**, L371 (2005). doi:10.1088/0305-4470/38/21/L01
3. Niven, R.K.: Phys. Rev. E **80**, 021113 (2009)
4. Dewar, R.C.: Entropy **11**(4), 931 (2010)
5. Niven, R.K.: Phil. Trans. R. Soc. B **365**, 1323 (2010)
6. Ozawa, H., Ohmura, A., Lorenz, R.D., Pujol, T.: Rev. Geophys. **41**, 1018 (2003)

7. Kleidon, A., Lorenz, R.D. (eds.): Non-Equilibrium Thermodynamics and the Production of Entropy: Life, Earth, and Beyond. Springer, Heidelberg (2005)
8. Kleidon, A. Malhi, Y. Cox, P.M.: Phil. Trans. R. Soc. B **365**, 1297 (2010)
9. Lorenz, R.D. Lunine, J.I., Withers, P.G. McKay, C.P.: Geophys. Res. Lett. **28**, 415 (2001)
10. Lorenz, R.D., Mckay, C.P.: Icarus **165**(2), 407 (2003)
11. Kleidon, A., Fraedrich, K., Kunz, T., Lunkeit, F.: Geophys. Res. Lett. **30**, 2223 (2003). doi:10.1029/2003GL018363
12. Kleidon, A., Fraedrich, K., Kirk, E., Lunkeit, F.: Geophys. Res. Lett. **33**, L06706 (2006). doi:10.1029/2005GL025373
13. Goody, R.: J. Atmos. Sci. **64**, 2735 (2007)
14. Volk, T.: Clim. Ch. **85**, 251 (2007)
15. Volk, T., Pauluis, O.: Phil. Trans. R. Soc. B **365**, 1317 (2010)
16. Kiehl, J.T., Trenberth, K.E.: Bull. Amer. Meteorol. Soc. **78**, 197 (1997)
17. Kleidon, A.: Phil. Trans. R. Soc. A **370**, 1012 (2012)
18. Kleidon, A.: Clim. Ch. **66**, 271 (2004)
19. Schneider, E.D., Kay, J.J.: Math. Comput. Modeling **19**, 25 (1994)
20. Kleidon, A., Zehe, E., Ehret, U., Scherer, U.: Hydrol. Earth Syst. Sci. **17**, 225 (2013)
21. Hansen, J., Lacis, A., Rind, D., Russell, G., Stone, P., Fung, I., Ruedy, R., Lerner, J.: Climate processes and climate sensitivity. Geophys. Monogr. **29** (1984), (American Geophysical Union)
22. Malkus, W.V.R.: Phys. Fluids **8**, 1582 (1996)
23. Lorenz, E.N.: Tellus **7**, 157 (1955)
24. Lorenz, E.N.: Dynamics of Climate. In: Pfeffer, R.C. (ed.) pp. 86–92. Pergamon Press, Oxford (1960)
25. Pauluis, O., Held, I.M.: J. Atmos. Sci. **59**, 126 (2002)
26. Pauluis, O., Held, I.M.: J. Atmos. Sci. **59**, 140 (2002)
27. Pauluis, O.: Water vapor and entropy production in the Earth's atmosphere. In: Kleidon, A., Lorenz, R. D. (eds.) Non-Equilibrium Thermodynamics and the Production of Entropy: Life, Earth, and Beyond, pp. 173–190, Springer, Heidelberg (2005)
28. Kleidon, A., Renner, M.: Hydrol. Earth Syst. Sci. 17, 2873–2892 (2013), doi:10.5194/hess-17-2873-2013
29. Lovelock, J.E.: Nature **207**, 568 (1965)
30. Lovelock, J.E.: Proc. Roy. Soc. Lond. B **189**, 167 (1975)
31. Juretic, D., Zupanovic, P.: The free-energy transduction and entropy production in initial photosynthetic reactions. In: Kleidon, A., Lorenz, R. D. (eds.) Non-Equilibrium Thermodynamics and the Production of Entropy: Life, Earth, and Beyond, pp. 161–172, Springer, Heidelberg (2005)
32. Lotka, A.J.: Proc. Natl. Acad. Sci. U.S.A. **8**, 147 (1922)
33. Lotka, A.J.: Proc. Natl. Acad. Sci. U.S.A. **8**, 151 (1922)
34. Prigogine, I.: Science **201**, 777 (1978)
35. Bejan, A., Lorente, S.: Phil. Trans. R. Soc. B **365**, 1335 (2010)
36. West, G.B., Brown, J.H., Enquist, B.J.: Science **276**, 122 (1997)
37. Kleidon, A.: Phys. Life Rev. **7**, 424 (2010)